L characteristic length defined by $L^2 = L_c L_{c1}$, m
$\mathbf{n}_{\beta\sigma}$ $-\mathbf{n}_{\sigma\beta}$, unit normal vector directed from the β-phase toward the σ-phase
$\mathbf{O}$ Order-of-magnitude symbol
t time, s
t^* characteristic process time, s
$\mathscr{V}$ averaging volume, m^3
V_β volume of the β-phase contained in the averaging volume, m^3
V_σ volume of the σ-phase contained in the averaging volume, m^3

Greek Letters

α_1 equilibrium coefficient
α_2 reaction rate parameter, moles-s m^{-3}
α_3 reaction rate parameter, s
α_4 reaction rate parameter, s
α_5 reaction rate parameter, m^3s $moles^{-1}$
ε_β volume fraction of the β-phase ($=V_\beta/\mathscr{V}$)
ε_σ volume fraction of the σ-phase ($=1-\varepsilon_\beta$)
ψ dimensionless parameter defined by Eq. (26) or Eq. (27)
κ dimensionless parameter defined by Eq. (26) or Eq. (27)
ρ_σ density of the σ-phase, kg m^{-3}
$\langle\rho_\sigma\rangle^\sigma$ intrinsic average σ-phase density (mass of cells per unit volume of cells), kg m^{-3}
$\langle\rho_\sigma\rangle$ superficial average σ-phase density ($=\varepsilon_\sigma\langle\rho_\sigma\rangle^\sigma$), kg m^{-3}
μ_A maximum specific substrate utilization rate parameter, moles m^{-3} s^{-1}
μ'_{eff} effective maximum specific substrate utilization rate parameter, pseudo one-equation model [defined by Eq. (17)], mol kg^{-1} s^{-1}
μ_{eff} effective maximum specific substrate utilization rate parameter, one-equation equilibrium model [defined by Eq. (19)], mol kg^{-1} s^{-1}
$\mu'_{eff,pseudo}$ effective maximum specific substrate utilization rate parameter, pseudo one-equation model [defined by Eq. (24)], mol m^{-2} s^{-1}
Γ membrane kinetic rate term ($=\alpha_2+\alpha_3\langle c_{A\beta}\rangle^\beta+\alpha_4\langle c_{A\sigma}\rangle^\sigma+\alpha_5\langle c_{A\beta}\rangle^\beta\langle c_{A\sigma}\rangle^\sigma$), mol-s m^{-3}.

Acknowledgments

The first author received support from the Department of Health and Environmental Research (EMSL Intermediate Flow Cells project), U.S. Department of Energy, and from the ECRI LDRD program at Pacific Northwest National Laboratory. Pacific Northwest Laboratory is operated for the U.S. Department of Energy by Battelle Memorial Institute under contract DE-AC06-76RLO 1830.

[23] Limiting-Current-Type Microelectrodes for Quantifying Mass Transport Dynamics in Biofilms

By ZBIGNIEW LEWANDOWSKI and HALUK BEYENAL

Overview

Quantifying factors affecting mass transport in biofilms help in understanding the mechanics of biofilm processes. Nutrients are delivered to the microorganisms embedded in extracellular polymers by mass transport and waste products are removed the same way. Since biofilm thickness is conveniently expressed in microns, the tools to study the intrabiofilm mass transport dynamics have to provide comparable resolution. We use microelectrodes, often in conjunction with confocal scanning laser microscopy. Although the use of microelectrodes for measuring concentration profiles of various substances in biofilms is well known, quantifying factors affecting mass transport in biofilms define a set of new challenges for making these measurements. These challenges are determined by the fact that the measured parameters are not simple physical quantities (e.g., oxygen concentration) but complex ones (e.g., mass transport coefficient or effective diffusivity) that appear as proportionality constants in respective equations describing mass transport dynamics. To evaluate these parameters the entire measurement system has to be designed in such way that the microelectrode response reflects the magnitude of these complex parameters. This chapter demonstrates the use of microelectrodes for evaluating the mass transport coefficient, effective diffusivity, and flow velocity in space occupied by biofilms.

Many of the concepts and all of the experimental results presented here were generated by the Biofilm Structure and Function Research Group at the Center for Biofilm Engineering. There are many excellent measurements of mass transport in biofilms reported by other research groups; however, limited space only allows referring to those that can be directly compared with our techniques. At several places in the text we indicate the types of instruments we use. This is not meant as an endorsement or recommendation of any specific piece of hardware, because many other instruments and tools are available that perform the same functions. Specifying what we use should serve as guidance, a point of departure for those intending to build such measurement systems.

Microelectrodes for Quantifying Factors Affecting Mass Transport in Biofilms

Microelectrodes are often used to measure local nutrient concentration profiles across biofilms.[1–3] The most commonly evaluated parameters of such profiles are

0076-6879/00 $35.00

the fluxes of nutrients consumed by the biofilm, e.g., oxygen, which are calculated by multiplying the slope of the concentration profile at the biofilm surface by the molecular diffusivity of the respective nutrient. However, difficulties arise in interpreting the results of such measurements. For instance, the shape of the nutrient concentration profile is affected by many factors, the most influential being those that affect mass transport dynamics (mass transport coefficient, effective diffusivity, hydrodynamics) and biofilm activity (substrate concentration, presence of inhibitory substances).[4] If the biofilm respiration rate or the flow velocity increase, the overall effect is the same: mass transport rate to the biofilm increases. At the macro scale of observation, it is not possible to distinguish the effects of mass transport dynamics from the effects of microbial activity on the overall nutrient consumption rate of the biofilm. Because biofilm reaction rates are generally limited by mass transport rates, an increase in flow velocity and an increase in microbial respiration rate both produce steeper nutrient concentration gradients.

To gain an insight into the dynamics of biofilm processes, microelectrode measurements of nutrient concentration profiles are often supplemented by the measurements of factors affecting mass transport dynamics. Combining results of these two groups of measurements allows us, in simple experimental systems, to distinguish the effects of mass transport from the effects of microbial activity on the overall biofilm activity. Although other procedures to evaluate the parameters characterizing mass transport in biofilms are available—microinjections combined with confocal scanning laser microscopy[5,6] and fluorescent recovery after photobleaching[7] (FRAP)—using microelectrodes to quantify mass transport dynamics is often the superior method because it can be integrated with the microelectrode measurements of nutrient concentration profiles. The purpose of this chapter is to demonstrate the utility of the limiting-current-type microelectrodes for quantifying factors affecting mass transport in biofilms.

Quantifying the factors affecting mass transport in biofilms is complicated by the fact that biofilms are structurally heterogeneous, i.e., microorganisms in biofilms are clustered in microcolonies separated by voids.[8–12] As a consequence,

[1] N. P. Revsbech, *J. Microbiol. Meth.* **9**, 11 (1989).
[2] Z. Lewandowski, G. Walser, and W. G. Characklis, *Biotechnol. Bioeng.* **38**, 877 (1991).
[3] Y. C. Fu, T. C. Zhang, and P. L. Bishop, *Wat. Res.* **29**, 455 (1994).
[4] K. Rasmussen and Z. Lewandowski, *Biotechnol. Bioeng.* **59**, 302 (1998).
[5] D. de Beer, P. Stoodley, and Z. Lewandowski, *Biotechnol. Bioeng.* **53**, 151 (1997).
[6] J. R. Lawrence, G. M. Wolfaardt, and D. R. Korber, *Appl. Environ. Microbiol.* **60**, 1166 (1994).
[7] J. D. Bryers and F. Drummond, *Biotechnol. Bioeng.* **60**, 562 (1998).
[8] D. de Beer, P. Stoodley, and Z. Lewandowski, *Biotechnol. Bioeng.* **44**, 636 (1994).
[9] D. de Beer, P. Stoodley, F. Roe, and Z. Lewandowski, *Biotechnol. Bioeng.* **43**, 1131 (1994).
[10] D. R. Noguera, S. Okabe, and C. Picioreanu, *Wat. Sci. Tech.* **39**, 273 (1999).
[11] P. L. Bishop and B. E. Rittmann, *Wat. Sci. Tech.* **32**, 263 (1995).
[12] J. R. Lawrence, D. R. Korber, B. D. Hoyle, J. W. Costerton, and D. E. Caldwell, *J. Bacteriol.* **173**, 6558 (1991).

chemistries and mass transport rates vary among points in the biofilm,[13–15] and measuring a single concentration profile at an arbitrarily selected location cannot describe the complex, three-dimensional effects of mass transport dynamics on biofilm activity. It is apparent that more complex protocols must be applied for such measurements.

In our laboratory, we have developed tools and experimental protocols to measure parameters that quantify factors affecting mass transport dynamics in three dimensions, as well as to generate maps of the spatial distribution of the measured parameters in biofilms. Although using these protocols made studying the mass transport in heterogeneous biofilms in three dimensions possible, it also makes the interpretation of the results complex because they are in three dimensions and because there are no simple mathematical models available to facilitate this process.

Factors affecting mass transport in biofilms can be monitored at two levels of observation: macro and micro scale. It is difficult to prescribe a specific dimension separating these scales of observation because any magnitude selected to separate them would have to be chosen arbitrarily. Therefore, it is better to base such distinction on what is expected from each scale of observation and what tools are routinely applied at the macro and micro scale. Macro-scale observations refer to the average overall properties of the entire system measured by chemical analysis of the bulk solution with the aid of mass balances. Micro-scale observations refer to the spatial distribution of factors affecting the local microbial activity and the local mass transport dynamics, e.g., local biofilm structure, local hydrodynamics, and local mass transport rates. Tools used for micro-scale observations must principally provide resolution high enough to distinguish the distribution of the measured quantities at a scale comparable with the smallest dimension of the biofilm—biofilm thickness. A variety of microscopy and microsensor tools can provide the micron-sized resolution necessary for these measurements.

Results generated at the micro scale are difficult to compare with results generated at the macro scale. Clearly, the effects measured at the macro scale have to be related to the underlying biofilm processes taking place at the micro scale. It is a major challenge in biofilm engineering to integrate the results of the micro-scale observations for predicting the results measured at the macro scale. Thus far these efforts of "scaling up" the micro-scale observations have not been very successful, demonstrating that our knowledge of biofilm processes is still inadequate.

For system analysis, it is convenient to subdivide the space influenced by biofilm activity into two zones: external (the bulk solution) and internal (the biofilm). Micro-scale measurements of mass transport dynamics in both external and internal zones of bacterial biofilms are the subject of this chapter. To simplify

[13] B. R. Rittmann, M. Pettis, W. H. Reeves, and D. Stahl, *Wat. Sci. Tech.* **39**, 99 (1999).
[14] C. Picioreanu, M. C. M. van Loosdrecht, and J. J. Heijnen, *Biotechnol. Bioeng.* **57**, 718 (1998).
[15] C. Picioreanu, M. C. M. van Loosdrecht, and J. J. Heijnen, *Biotechnol. Bioeng.* **58**, 101 (1998).

the considerations, we assume that (1) the mass transport dynamics in the external zone is entirely defined by the bulk liquid hydrodynamics, and also that there is no substrate consumption in that zone, and (2) the mass transport dynamics in the internal zone is entirely defined by the intrabiofilm hydrodynamics, by biofilm structure, and by biofilm activity.

Limiting Current and Limiting-Current-Type Sensors

The limiting-current-type sensors belong to a large group of amperometric sensors whose principle use is measuring current generated by reducing (or oxidizing) electroactive materials at surfaces of electrically polarized electrodes.[16] The current measured by these devices is equivalent to the rate of the electrode reaction, which is determined by the applied potential and the rate at which the reactant arrives at the electrode (mass transport rate). In this reaction, increasing the potential increases the current up to a point termed "limiting current" beyond which any further increase of the potential does not produce more current. This condition exists because the reaction rate is now determined by the rate at which the electroactive material arrives at the electrode, i.e., the mass transport rate. Factors determining the rate are diffusivity of the material surrounding the electrode, bulk liquid reactant concentration, and hydrodynamics.

The amperometric microelectrodes used for measuring concentrations of selected nutrients in biofilms (e.g., oxygen) are covered with membranes that determine the mass transport resistance of the measured substance to the electrode. In principle, such microelectrodes are not sensitive to the conditions determining the mass transport rate of the measured substance in the bulk solution (e.g., flow rate), because the majority of mass transport resistance to the microelectrode is confined within the membrane. In other words, the membrane shields the device from the variations in external mass transport rates. To better quantify factors affecting mass transport dynamics in biofilms, we use amperometric sensors without membranes, which makes them sensitive to the mass transport rates in the solution. As long as the bulk-liquid reactant concentration remains constant, the limiting current measured by such devices depends strictly on the mass transport rate of the electroactive material to the microelectrode. Devices that build on the limiting current principle are well known for determining mass transport rates and studying the effects of hydrodynamics on mass transport rates in various systems.[17–21] Two differences distinguish our sensors from those described in the literature: our sensors have tip diameters less than 10 μm, and they are mobile.

[16] T. Mizushina, *Adv. Heat Transfer* 7, 87 (1971).
[17] S. Yapici, M. A. Patrick, and A. A. Wragg, *J. Appl. Electrochem.* 24, 685 (1994).
[18] N. M. Juhasz and W. M. Deen, *AIChE. J.* 39, 1708 (1993).
[19] S. J. Konopka and B. McDuffie, *Anal. Chem.* 42, 1741 (1970).
[20] P. H. Vogtlander and C. A. P. Bakker, *Chem. Eng. Sci.* 18, 583 (1963).
[21] W. E. Ranz, *AIChE. J.* 4, 338 (1958).

To apply the limiting-current-type microelectrodes in biofilm systems, two conditions need to be satisfied: (1) the only sink for the electroactive substance must be the microelectrode tip and (2) there can be only one electroactive substance available for the electrode to process at a time. After a suitable electroactive substance has been selected and introduced to a biofilm, a microelectrode, polarized to an extent that satisfies the limiting current conditions, reduces (or oxidizes, depending on the procedure) this substance. The electroactive substance is then locally removed (converted to another substance) at the tip of the microelectrode, thereby locally decreasing the concentration of this substance in the vicinity of the microelectrode tip. After a few seconds, an equilibrium is established between the rate at which the electroactive substance is locally removed by the electrode reaction and the rate at which it is supplied by the mass transport. The limiting current reflects the position of this equilibrium. If, for any reason, the rate of mass transport of the electroactive substance to the tip of the microelectrode changes, the limiting current changes. For our experiments we use mobile microelectrodes and expose their tips at various locations in biofilms. As the electroactive reactant we use a 25 m*M* solution of potassium ferricyanide, $K_3Fe(CN)_6$, in 0.2 *M* KCl. With proper experimental control, the ferricyanide is reduced to ferrocyanide, $Fe(CN)_6^{4-}$, at the surface of cathodically polarized microelectrodes:

$$Fe(CN)_6^{3-} + e^- \rightarrow Fe(CN)_6^{4-} \qquad (1)$$

Increasing the polarization potential applied to the microelectrode increases the rate of the electrode reaction (that is, the rate of reduction of ferricyanide to ferrocyanide) until the rate reaches its limit for the existing set of conditions. At limiting current, the concentration of ferricyanide at the electrode surface is zero, and the concentration gradient cannot increase any further. Figure 1 shows a microelectrode immersed in a solution of ferricyanide, polarized with respect to a reference electrode, and measuring limited current. For such conditions, the concentration of ferricyanide at the electrode surface is zero ($C_s = 0$) while in the bulk solution it remains C_0. The concentration gradient is said to be confined entirely within the mass transfer boundary layer, δ. The flux of the ferricyanide, J, to the exposed surface of the microelectrode with the sensing area, A, is related to the limiting current, I, by Eq. (2):

$$J = \frac{I}{nAF} \qquad (2)$$

Here F is Faraday's constant, and n is the number of electrons transferred in the balanced reaction. For practical reasons, the results of current measurement are reported as limiting current density, (I/A), which describes the ratio of the limiting current to the reactive surface area of the microelectrode tip. The flux of ferricyanide to the electrode can also be expressed as Fick's first law:

$$J = \frac{D(C_0 - C_s)}{\delta} = k(C_0 - C_s) \qquad (3)$$

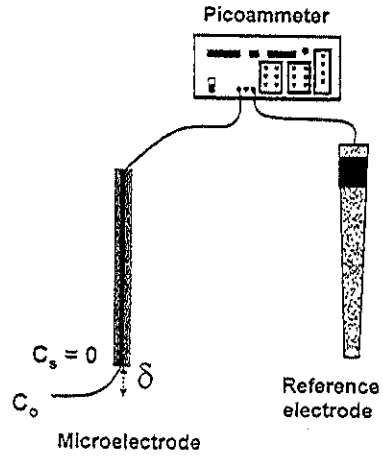

FIG. 1. At limiting current, ferricyanide concentration at the electrode surface is zero ($C_s = 0$) while the concentration of ferricyanide in the bulk solution remains C_0. Concentration gradient is confined within the boundary layer of δ thickness.

Here, D is the diffusivity of ferricyanide; concentration of the ferricyanide in the bulk solution is C_0, and at the surface of the microelectrode it is C_s; k is the mass transport coefficient; and δ designates the thickness of the diffusion boundary layer, controlled by the local shear stress and flow velocity.[16,22–25] In stagnant water, δ is controlled only by the diffusivity of ferricyanide.[26–28] A properly arranged experimental system using a mobile microelectrode allows for measuring rates of transport of ferricyanide to the microelectrode tip, and this transport rate is equivalent of the nutrient transport rate in biofilms at that location.

We use several modes of measurements to quantify factors influencing mass transport dynamics in biofilms. The simplest to measure is the local mass transfer coefficient.[29] More complicated are local effective diffusivity[30,31] and local flow

[22] T. J. Hanratty and J. A. Campbell, *in* "Fluid Mechanics Measurements" (R. J. Goldstein, ed.), p. 616. Taylor and Francis, Washington, D.C., 1996.
[23] J. R. Selman and C. W. Tobias, *in* "Advances in Chemical Engineering" (B. Drew, G. R. Cokelet, J. W. Hoopes, and T. Vermeulen, Jr., eds.), p. 211. Academic Press, New York, 1978.
[24] H. G. Dimopoulos and T. J. Hanratty, *Fluid. Mech.* 33, 303 (1968).
[25] J. A. Campbell and T. J. Hanratty, *AIChE. J.* 28, 988 (1982).
[26] X. Gao, J. Lee, and H. S. White, *Anal. Chem.* 67, 1541 (1995).
[27] C. Amatore and B. Fosset, *Anal. Chem.* 65, 2311 (1993).
[28] Z. Galus and J. Osteryoung, *J. Phys. Chem.* 92, 1103 (1988).
[29] S. Yang and Z. Lewandowski, *Biotechnol. Bioeng.* 48, 737 (1995).
[30] H. Beyenal, A. Tanyolaç, and Z. Lewandowski, *Wat. Sci. Tech.* 38, 171 (1998).
[31] H. Beyenal and Z. Lewandowski, *Wat. Res.* 34, 528 (2000).

velocity.[32] The greatest benefits of these measurements can be expected when the results are compared with the local nutrient consumption rates measured by other microelectrodes. Such a combination gives us an image of the relations between local mass transport dynamics and local microbial activity. Since application of limiting-current-type sensors requires introducing ferricyanide, which inactivates metabolic reactions in biofilms, measurements of mass transport dynamics have to be conducted separately for the measurement of the primary substrate utilization rate by the biofilm. Local substrate utilization rates are measured first, then the nutrient solution is replaced by the electrolyte and the factors affecting mass transport dynamics are quantified. It has been demonstrated that replacing the nutrient solution with the electrolyte does not change the biofilm structure.[29] To combine the results of local microbial respiration rate and local mass transport dynamics, the microelectrode measurements have to be conducted at exactly the same location, which is a challenging task. To find the location using different microelectrodes, we grow biofilms on microscope coverslips that are marked with a grid (Fisher Scientific). The slides are positioned at the bottom of the flat plate reactor, and the exact location for microelectrode measurements is then found using the inverted microscope positioned below the reactor (Fig. 2).

Technically, all microelectrode measurements are similar: a cathodically polarized microelectrode measures the limiting current at different locations in a biofilm. The differences in experimental conditions and the differences in microelectrode calibration procedures define what is actually measured. For example: to measure a local mass transfer coefficient, the measurements are conducted in flowing electrolyte because the convective mass transport component needs to be included in the final result. To measure local effective diffusivity we use the same system, but the flow is stopped and the measured limiting current reflects only the diffusional component of mass transport. In the former case the electrode is not calibrated; however, in the latter case the microelectrode has to be calibrated using gels of known densities and effective diffusivities.

The mass transfer coefficient can be found[29] by solving Eqs. (2) and (3) for $C_s = 0$.

$$k = \frac{I}{nAFC_0} \tag{4}$$

If the current is measured directly and all other factors are known, the mass transport coefficient is calculated from Eq. (4). The surface area of the microelectrode needs to be known *a priori*, but the microelectrodes that measure the mass transport coefficient do not need to be calibrated.

In contrast, microelectrodes used to measure effective diffusivity need to be calibrated. The reason that the local effective diffusivity cannot be directly

[32] F. Xia, H. Beyenal, and Z. Lewandowski, *Wat. Res.* 32, 3637 (1998).

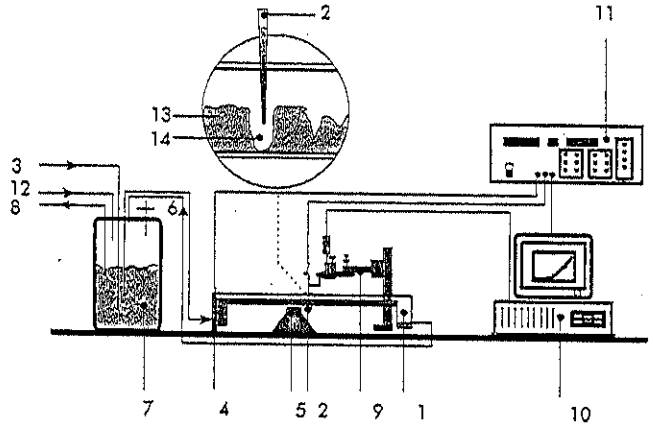

FIG. 2. Experimental setup used to grow biofilms and perform microelectrode measurements: 1, open channel, flat plate reactor; 2, microelectrode; 3, air conduit; 4, reference electrode; 5, inverted microscope/confocal scanning laser microscope; 6, air filter; 7, mixing chamber; 8, effluent; 9, micromanipulator; 10, data acquisition system; 11, picoammeter/DC voltage source; 12, fresh feed conduit; 13, biofilm cluster; 14, biofilm void.

calculated from Eq. (3) is that the limiting current depends on the thickness of the diffusion boundary layer, δ, around the microelectrode tip. However, this value is unknown and depends on the diffusivity, D, in a stagnant solution. For that reason microelectrodes used to measure effective diffusivity have to be calibrated in gels with characteristics similar to those of the extracellular biopolymers in biofilms and of known effective diffusivities.

Microelectrodes used to measure local flow velocity have to be calibrated as well. The major factor defining mass transport rates in the flowing electrolyte is convection, which makes it possible to quantitatively relate the limiting current measured by microelectrodes in ferricyanide solution to local flow velocities in the vicinity of the microelectrode tip. We have tested that the procedure works at low and very low velocities not exceeding a few centimeters per second. To calibrate such microelectrodes, the local flow velocities in the vicinity of the microelectrode tip are measured using velocimetry combined with confocal scanning laser microscopy as described later in this chapter.

Procedures

Growing Biofilms

An open channel biofilm reactor (Fig. 2) made of transparent polycarbonate, 2 cm deep, 4 cm wide, and 75 cm long, is used.[29] The nutrient solution consists of

KH_2PO_4 (2.2 m*M*), K_2HPO_4 (4.8 m*M*), $(NH_4)SO_4$ (0.25 m*M*), $MgSO_4$(0.04 m*M*), and yeast extract (0.01 g/liter), and it is recycled through the reactor at a rate of 10 ml/s by a magnet driven vane pump (Cole-Parmer, Chicago, IL). Oxygen is supplied by preaerating the nutrient solution. The operating volume of the recycle loop, including the reactor, is 450 ml. The inoculum consists of *Pseudomonas aeruginosa* (ATCC 700829), *Pseudomonas fluorescens* (ATCC 700830), and *Klebsiella pneumoniae* (ATCC 700831). After inoculation, the reactor is operated as a batch for 12 hr, and then in a continuous flow mode. Nutrient solution is added by a peristaltic pump (Masterflex; Cole-Parmer, Niles, IL) at a rate of 15 ml/min to achieve a hydraulic residence time of 30 min. A short retention time prevents buildup of suspended growth. The biofilm is allowed to grow for 4 to 7 days before the measurements are taken.

Replacing Nutrients with Electrolyte

Just before the measurements are taken, the nutrient delivery is interrupted and the nutrient solution is slowly drained from the reactor and replaced with the electrolyte solution properly formulated for the measurements: 25 m*M* $K_3Fe(CN)_6$ in 0.2 *M* KCl. When measurements of mass transport parameters are conducted in flowing electrolyte, the solution is recycled through the biofilm reactor using a gravitational flow system to ensure that the flow rate is constant and without pulsation. Flow rates are adjusted by a control valve and continuously monitored by a flowmeter (Model GF-1500, Gilmont Instruments, Barrington, IL). The recirculating electrolyte is filtered through a quartz wool plug to remove large aggregates of cells. As a final step prior to the measurements, the electrolyte solution is allowed to flow through the biofilm reactor for at least 30 min to equilibrate with the biomass.

Constructing and Testing Microelectrodes

To make the microelectrodes, we use a platinum wire (California Wire Company, Grover Beach, CA), 100 μm in diameter (pure TC grade). The tip of the wire is etched electrochemically (7 volts AC against graphite counterelectrode) to a diameter between 2 and 6 μm in a saturated KCN solution. The wire is rinsed with distilled water and carefully inserted into a capillary made of soda-lime glass. The capillary is positioned in a microelectrode puller (Stoelting Co., Wood Dale, IL) in such way that the tip of the platinum wire is about 1.5 cm above the heating coil. The heat is slowly increased until the glass around the platinum wire melts and adheres to the wire, while the entire capillary drops down, separates, and cools in the air. The tip of the wire is then exposed by grinding it on a rotating diamond wheel (Model EG-4, Narishige Co., Tokyo) and then cleaned in a sonication bath, first in distilled water, then in acetone. The diameter of the microelectrode tip is measured under a microscope, and its surface area is then calculated. To prevent

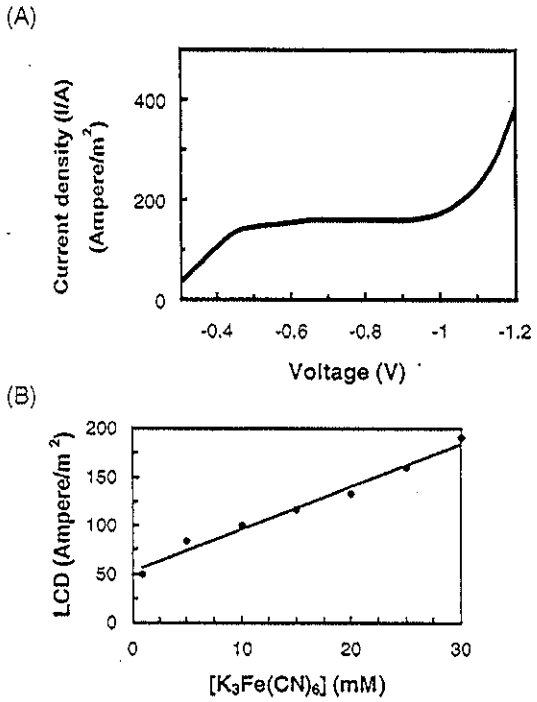

FIG. 3. (A) A polarization curve for a microelectrode tip diameter 10 μm in an unstirred solution of 25 m*M* $K_3Fe(CN)_6$ in 0.2 *M* KCl. (B) The limiting current is linearly correlated with the bulk water ferricyanide concentration, demonstrating that the reaction at the tip of the microelectrode is truly diffusion controlled.

damaging the biofilm structure, we use electrodes with an outside tip diameter less than 10 μm. The electrical connection with the external circuit is made by inserting a small piece of solder wire and a bare copper wire into the capillary and melting the solder in a stream of hot air to form a metallic droplet connecting the platinum and the copper wires. A voltammetry test is performed on each microelectrode to check its performance. The polarization potential is scanned from 0.0 to −1.2 V in a solution of 0.2 *M* KCl and 25 m*M* potassium ferricyanide, $K_3Fe(CN)_6$. Potassium chloride, KCl, is used as supporting electrolyte to suppress the contribution of electromigration to the microelectrode.[23,29] The microelectrodes having stable limiting current in the voltage range between −0.6 and −0.9 V are considered usable (see Fig. 3A). The actual concentrations of $Fe(CN)_6^{3-}$ are determined by iodimetric titration before each measurement.[33] Occasionally, the dependence of

[33] A. Vogel, "A Textbook of Quantitative Inorganic Analysis Including Elementary Instrumental Analysis." Longman, London, 1978.

the limiting current on the ferricyanide concentration is tested; if it is linear, it confirms that the reaction at the tip of the microelectrode is truly diffusion controlled[34] (see Fig. 3B).

As reference/counterelectrodes we use commercial calomel electrodes (Model 13-620-51, Fisher Scientific, Pittsburgh, PA). A Hewlett Packard 4140B multimeter is used as a voltage source and picoammeter. During the biofilm measurements the microelectrodes are polarized cathodically to −0.8 V against the reference electrode, which is placed next to it within the reactor in the downstream direction.

Figure 3A shows typical results of microelectrode testing. When the applied potential increases from 0 to −0.5 V, current increases as well. For potentials between approximately −0.6 and −1.0 V, the current remains constant, which reflects the limiting current conditions. As a rule, if the current is stable between −0.6 and −0.9 V, the tested microelectrode is accepted. Increasing the potential beyond −1.0 V causes chemical reduction of water, an additional reaction that increases the current. Based on the results similar to those in Fig. 3A, we decided to polarize the microelectrodes at −0.8 V during the measurements in biofilm rectors. Since at −0.8 V oxygen can be reduced, we have considered the need for removing oxygen from the system prior to taking the measurements. However, tests demonstrated that the limiting current generated by reducing ferricyanide to ferrocyanide was not affected by the presence of oxygen. Two reasons may, hypothetically, explain this result: (1) the concentration of ferricyanide in the system, 25 m*M*, exceeds the solubility of oxygen in water, 0.5 m*M*, by a factor of 50, and (2) the reduction of ferricyanide is kinetically preferred.

An important condition that needs to be satisfied by measuring systems using limiting-current-type microelectrodes is that the electrode reaction must be the only sink (or source) of electrons for the selected electroactive substance. This condition prevents using some convenient cathodic reactants, such as oxygen, as electroactive materials for limiting current measurements in biofilms. The reason is that oxygen would be reduced by the microorganisms, and the electrode reaction would not be the only source of electrons to reduce oxygen. Effectively, in such a system the microelectrode would compete for oxygen with the microorganisms.

The condition that the electrode reaction is the only sink (or source) of electrons needs to be verified for each selected reactant. For example, in our measurements the biomass can serve as a source of electrons to reduce ferricyanide, therefore competing with the electrode reaction. Our tests show that it takes at least 30 min for the ferricyanide to equilibrate with the biomass. To test if the system is equilibrated, we measure profiles of ferricyanide across the biofilm using ferricyanide microelectrodes. Ferricyanide microelectrodes are constructed in the same way as

[34] A. D. Dawson and O. Trass, *J. Heat Mass Transfer* 15, 1317 (1972).

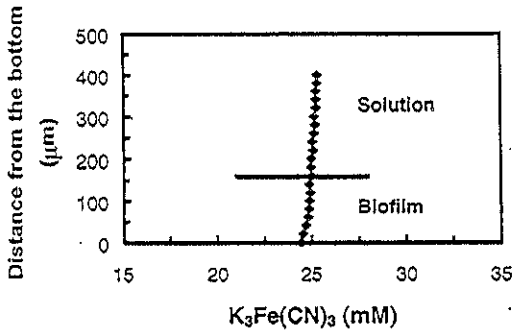

FIG. 4. Profiles of ferricyanide concentration measured to evaluate whether the system was already equilibrated. The ferricyanide in the bulk solution was 25 m*M* $K_3Fe(CN)_6$ in 0.2 *M* KCl. The slight decrease of the ferricyanide concentration near the bottom shows that the system may need more time to equilibrate.

the microelectrodes used to measure the mass transport dynamics, with one exception: we cover their tips with a 5% cellulose acetate membrane. An appropriate amount of cellulose acetate to make 5% solution is dissolved in acetone and the tip of the microelectrode dipped into the solution and dried overnight. The presence of the membrane makes the electrodes useless for measuring the mass transport coefficients, but makes them convenient tools to measure the concentration of ferricyanide within the biofilm.

Figure 4 shows results of such measurements in a biofilm that was equilibrated with the ferricyanide for 30 min. If the system is properly equilibrated, the concentration of ferricyanide across the biofilm does not change. The results in Fig. 4 show a slight bend on the profile just above the bottom, indicating that the system could benefit from having more time to equilibrate. For some measurements (e.g., in thick and dense biofilms) we equilibrate the system for 2 hr.

Calibrating Effective Diffusivity Microelectrodes

To calibrate the effective diffusivity microelectrodes, we use agar gels of known effective diffusivities. To prepare such gels, one needs to determine the effective diffusivity of ferricyanide in agar gels of different densities. For that purpose we use a diffusion cell consisting of two tanks, each 11 cm deep, 10 cm wide, and 10 cm long, separated by a dialysis membrane (Spectrum, 132709, La Cadena, CA); a fresh membrane is used for each experiment. A suspension of agar (BBL 11853; Becton Dickinson Microbiology Systems, Cockeysville, MD) in 0.2 *M* KCl is heated to 100° (in boiling water), then cooled to 40–60° and carefully poured onto the dialysis membrane. The lower tank (1.040 liter working volume) is filled

with 25 m*M* $K_3Fe(CN)_6$ in 0.2 *M* KCl and stirred by a magnetic stirrer to avoid mass transport limitations to the membrane, while the upper tank (0.560 liter working volume) is filled with 0.2 *M* KCl. The ferricyanide diffuses from the lower tank through the membrane and the agar layer into the upper tank. The entire diffusion cell operates in a temperature controlled (25 ± °) water bath. The concentration of ferricyanide in the upper tank is measured spectroscopically at a wavelength of 430 nm. The effective diffusivity is measured both through the membrane alone and through the membrane and agar together, and the difference is used to calculate the effective diffusivity in agar. The procedure of calculating the effective diffusivity from such results is described in detail in Beyenal and Lewandowski.[31]

To prepare agar layers of known density and effective diffusivity, the known amount of agar is dissolved in a solution of $K_3Fe(CN)_6$ and 0.2 *M* KCl. The solution is slowly heated until the agar dissolves, then it is slowly cooled to 40–60° and poured as a layer 250–1000 μm thick on the bottom of the flat plate reactor (without biofilm). After the agar layer solidifies, the reactor is carefully filled with $K_3Fe(CN)_6$ in 0.2 *M* KCl electrolyte solution. The solution is recirculated for 2 hr to equilibrate the ferricyanide with the agar. Before the measurements are taken, the recycling process is stopped, and the solution remains stagnant for the duration of the measurements. The microelectrode is mounted on a micromanipulator (Model M3301L, World Precision Instruments, New Haven, CT), which is equipped with a stepper motor (Model 18503, Oriel, Stratford, CT), controlled by the Oriel Model 20010 interface, and introduced perpendicularly to the agar layer from the top of the reactor. The microelectrode is moved at a 20 μm step length across the agar layer, and the limiting current density, (I/A), is measured at different positions within the agar. The distance from the tip of the microelectrode to the bottom of the reactor is determined at each step. Figure 5A shows typical results of limiting current densities measured in agar gels of different densities and effective diffusivities.

Figure 5 shows that, in agar gels of constant density and constant effective diffusivity, the limiting current density is constant at a distance from the bottom of the reactor but decreases suddenly just above the bottom of the reactor. This variance is most likely because of the mass transfer limitations near the wall. This effect, also noticed by Beyenal *et al.*[30] and Yang and Lewandowski,[29] limits the application of microelectrodes at distances less than 60 μm from the bottom. Consequently, the results of the limiting current measurements closer than 60 μm from the bottom have to be ignored. The relation between the limiting current density measured by the microelectrodes and the effective diffusivity in the agar gel is linear within the range of tested agar densities (Fig. 5B). Using such calibration curves, the results of limiting current measurements can be expressed in terms of local effective diffusivities in the vicinity of the microelectrode tip at a selected location in the biofilm.

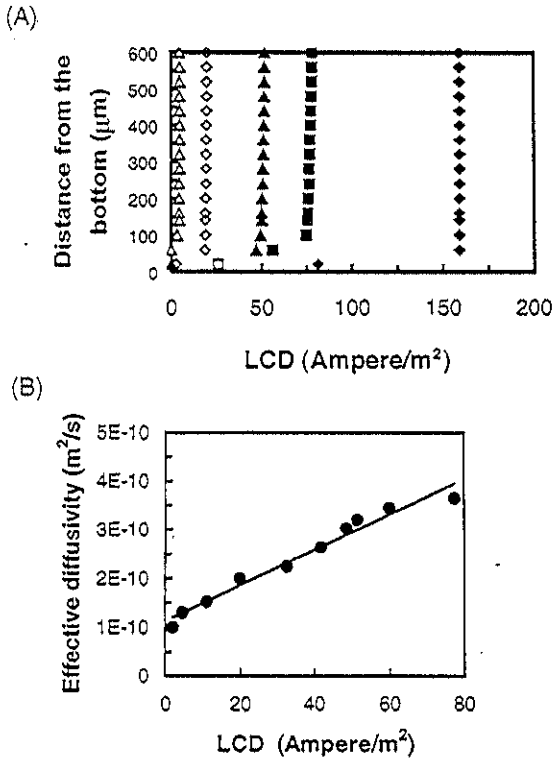

FIG. 5. (A) Limiting current density (LCD) in agar layers. ◆, Electrolyte solution. D_{ag} (m^2/s): ■, 3.66×10^{-10}; ▲, 3.21×10^{-10}; ◇, 1.98×10^{-10}; △, 1.29×10^{-10}. (B) The relation between the LCD and the effective diffusivity of ferricyanide within the range of tested agar densities and effective diffusivities. [Reproduced from H. Beyenal and Z. Lewandowski, *Wat. Res.* 34, 528 (2000).]

Calibrating Local Flow Velocity Microelectrodes

The limiting current microelectrodes respond to the rate of mass transport to the electrode tip. For flowing liquids the major factor that determines the mass transport rate is the thickness of the mass transfer boundary layer, which, in its turn, is determined by the local flow velocity (diffusivity of ferricyanide is constant). Since the response of the microelectrode depends on local flow velocity, we relate the limiting current measured by an ammeter to the local flow velocity. The difficult part here is determining the local flow velocity in a flow velocity field. We use the Bio-Rad model MRC600 confocal scanning laser microscope (CSLM) integrated with the Olympus model BH2 light microscope for particle tracking. Detailed procedures of the measurement of local flow velocities in biofilms are

given by Stoodley *et al.*[35] and De Beer *et al.*[8] Neutral-density fluorescent latex spheres [density at 20°, 1055 kg/m^3; excitation wavelength (Ex), 580 nm; emission wavelength (Em), 605 nm; diameter, 0.216 μm; Molecular Probes, Eugene, OR] are added to the reactor. Local velocity profiles in the reactor are obtained by raising or lowering the motorized stage and capturing images at different focal depths. The CSLM is used to capture images by using the Bio-Rad COMOS operating software. Particles traveling across the field of view appear as dashed lines. The velocity of a particle is calculated from the distance between the dashes and the time taken to scan the number of frame lines crossed by the particle. We then insert the microelectrode at the exact point where the CSLM images were taken and determine the limiting current. Principles of the calibration procedure are exemplified in Fig. 6.

Modes of Measurements and Interpretation of Results

Appropriate experimental setups are arranged in such way that the results of microelectrode measurements are collected as (1) profiles of local mass transport coefficients, effective diffusivities, or flow velocities across the biofilm, or (2) maps of spatial distribution of those parameters at different levels in the biofilm.

Profiles of Measured Parameters

The microelectrode is attached to a linear, computer-controlled micropositioner (Model CTC-322-20, Micro Kinetics) positioned above a selected location in the biofilm reactor. The micropositioner moves the electrode across the biofilm in predetermined intervals, e.g., 10 μm, taking measurement of the limiting current at each position. Figure 7 shows a profile of local mass transfer coefficients calculated from such results.[4]

Concentration profiles measured across the biofilm are site specific, meaning they are different at different locations (see Yang and Lewandowski[29]). Mathematical modeling of biofilms predicts biofilm activity over a certain surface. To verify biofilm models, the measurements need to evaluate an average biofilm activity over the same surface for which the activity was predicted using the model. Concentration profiles measured at different locations can show surprising variability, and it is not quite clear how to average these profiles. To quantify the extent of this variability, and to average the concentrations measured at different locations, it is often desirable to construct maps of concentration distribution at different levels in biofilms, instead of reconstructing concentration profiles across these biofilms.

[35] P. Stoodley, D. De Beer, and Z. Lewandowski, *Appl. Environ. Microbiol.* 60, 2711 (1994).

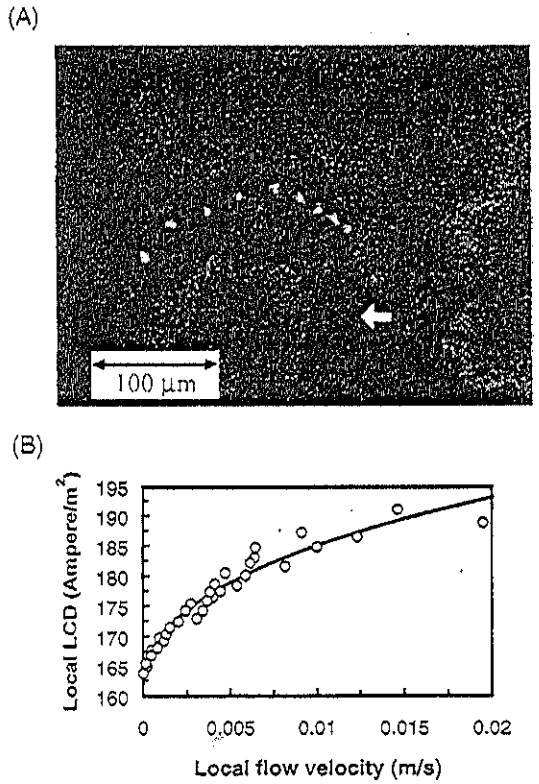

FIG. 6. Calibrating local flow velocity microelectrodes. (A) CSLM of fluorescent beads is used to measure local flow velocities. Reproduced from P. Stoodley, D. De Beer, and Z. Lewandowski, *Appl. Environ. Microbiol.* 60, 2711 (1994). (B) Local flow velocities correlated with the local limiting current density measurements indicate that for flow velocities not exceeding 2 cm/s, which are the flow velocities in the voids of many biofilms, the limiting current density correlates well with the local flow velocity. [Reproduced from F. Xia, H. Beyenal, and Z. Lewandowski, *Wat. Res.* 32, 3637 (1998).]

Maps of Spatial Distribution of Measured Parameters

To calculate the average mass transport coefficient and average effective diffusivity for the entire biofilm, we map spatial distribution of these parameters in the biofilm. Generating such maps is more complicated than reconstructing profiles of these parameters. To describe the spatial distribution of the measured parameters, and to find meaningful average mass transport coefficients and effective diffusivities, we use a different protocol from that used to measure profiles of these parameters. First, we design a grid above a selected part of the biofilm surface and make the measurements at the grid points. Second, instead of measuring the selected parameter across the biofilm in predesigned intervals (as is done when

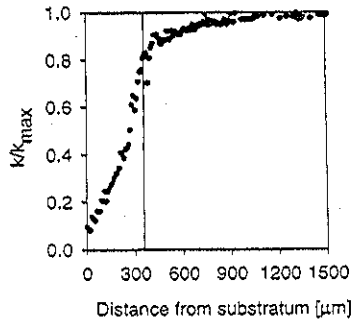

FIG. 7. Profile of the local mass transport coefficient across a cell cluster in a biofilm. The vertical line designates the approximate position of the biofilm surface. The results were normalized with respect to the maximum mass transport coefficient measured in the bulk solution. [Reproduced from K. Rasmussen and Z. Lewandowski, *Biotechnol. Bioeng.* 59, 302 (1998).]

measuring profiles), the linear micropositioner lowers the microelectrode to a preselected distance from the bottom of the reactor to make a single measurement. Then, the microelectrode is withdrawn from the biofilm, moved to the next grid point, and lowered to exactly the same distance from the bottom as for the previous measurement; another measurement is taken; and so on. Once these measurements are completed, we repeat the cycle of measurements at another distance from the bottom, using the same grid points. When all measurements are completed we have several sets of results of the measured parameters collected at selected distances from the bottom, and these values are then converted to maps of spatial distribution of the measured parameter at different levels in the biofilm. An advantage of this protocol is that such maps of spatial distributions of the measured parameters—local mass transfer coefficient, local effective diffusivity, and local flow velocity—at selected distances from the bottom are directly comparable with the CSLM images collected at the same distances from the bottom, making it possible to compare biofilm structure with the distribution of factors affecting mass transport dynamics.

For practical purposes, we use a combination of linear and *X–Y* micropositioners. The flat plate biofilm reactor is fixed to the *X–Y* micropositioner stage (Model CTC-462-2S, Micro Kinetics, Laguna Hills, CA), while the microelectrode is attached to the linear micropositioner (Model CTC-322-20, Micro Kinetics) positioned above the reactor. Both micropositioner are manipulated by a computerized controller (CTC-283-3, Micro Kinetics) with a positioning precision of 0.1 μm. Custom software is used to simultaneously control the *X–Y* stage movement, the microelectrode movement, and the data acquisition (Model CIO-DAS08PGL, Computer Boards, Inc., Mansfield, MA). For typical measurements a 10 × 10 grid matrix with a step size of 100 μm in both *X* and *Y* directions is used.

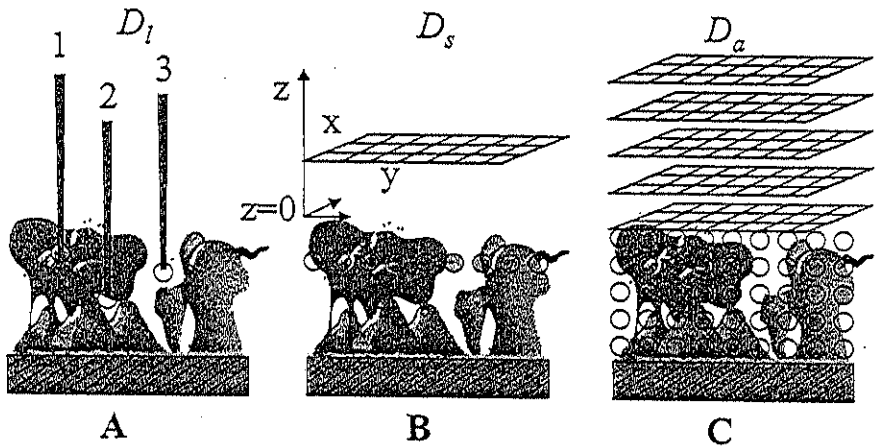

FIG. 8. A system of effective diffusivity measurements. (A) Local relative effective diffusivity (D_l) measured by microelectrodes at arbitrarily selected locations, and at different distances from the bottom. (B) The D_l values are measured at grid points equally distant from the bottom. The measured D_l values are then averaged, yielding the surface averaged relative effective diffusivity, $D_s = \sum_{n=1}^{k} D_{ln}/k$. (C) The average relative effective diffusivity, $D_a = \sum_{n=1}^{p} D_{sn}/p$, is the average of all local measurements for the entire biofilm. [Reproduced from H. Beyenal and Z. Lewandowski, *Wat. Res.* 34, 528 (2000).]

The microelectrode is manually positioned above the first grid point and the linear micropositioner moves the microelectrode into the biofilm to a predetermined distance from the bottom. After the limiting current has been measured and the data have been accepted, the linear micropositioner moves the microelectrode out of the biofilm and into the bulk liquid. The motorized *X–Y* stage moves the reactor to the next grid point, and then the linear micropositioner lowers the microelectrode to the same distance from the bottom as for the previous measurement. Maps of limiting current densities measured at the grid points equidistant from the bottom of the reactor are displayed on the computer's monitor in real time during the measurements. Figure 8 shows the experimental arrangement. Individual profiles of *local relative effective diffusivity*, D_l, vary from location to location and do not reveal the structured pattern of relative effective diffusivities found in biofilms (Fig. 8A). Local measurements are then arranged in a way that demonstrates that organization: we measure D_l at grid locations equidistant from the bottom and take the average of the results (Fig. 8B). The average of these D_l measurements is termed *surface averaged relative effective diffusivity*, D_s, and is different at different distances from the bottom. The set of these D_s averages contains as many individual results as the number of levels that were selected for effective diffusivity measurements. The average of all the D_l measurements taken at different distances from the bottom is termed *average relative effective diffusivity*, D_a, and represents the average effective diffusivity for the entire biofilm (Fig. 8C).

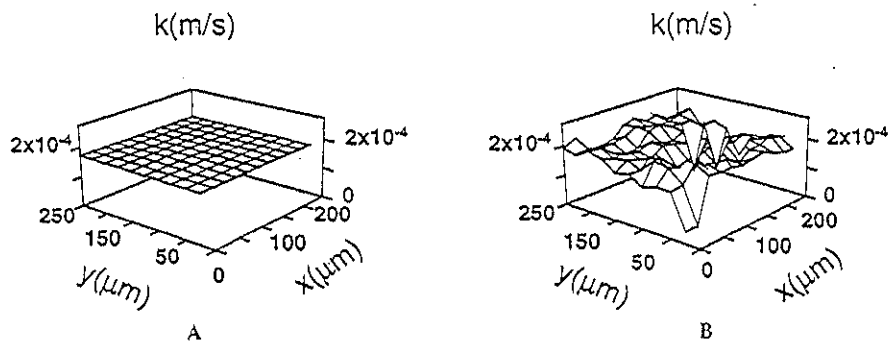

FIG. 9. Horizontal distributions of local mass transfer coefficient. Bulk flow velocity was 1.58 cm/s. Distances from the bottom: (A) $z = 1000$ μm (outside the biofilm), (B) $z = 200$ μm (inside the biofilm). [Reproduced from S. Yang and Z. Lewandowski, *Biotechnol. Bioeng.* 48, 737 (1995).]

When results are arranged as maps of spatial distribution, one can estimate average local mass transport coefficient and average local effective diffusivities at different levels within the biofilm over the surface area covered by the grid. Figure 9 shows typical results of such measurements: a map of mass transport coefficient distribution at selected levels above and within a biofilm.

Using this system of measurements one can, for example, quantify the effects of biofilm growth conditions on the average relative effective diffusivities in heterogeneous biofilms. For that purpose, we grow biofilms at different conditions, evaluate their average relative effective diffusivities, D_a, and present the results in a coordinate system that visualizes the effects of growth conditions on the average relative effective diffusivity. As an example, the effect of flow velocity and glucose concentration on average relative effective diffusivity of biofilms is visualized in Fig. 10.[31] The results show that concentration of glucose had a stronger effect on the average effective diffusivity than did flow velocity.

Local Biofilm Density

Biofilm density cannot be directly measured by microelectrodes. However, Fan *et al.*[36] suggested, based on extensive literature studies of the effective diffusivity measured in biofilms, activated sludge flocs, and mycelial pellets, the following empirical relation between average biofilm density and average relative effective diffusivity:

$$D_a = 1 - \frac{0.43 X_f^{0.92}}{11.19 + 0.27 X_f^{0.99}} \tag{5}$$

[36] L. S. Fan, R. L. Ramos, K. D. Wisecarver, and B. J. Zehner, *Biotechnol. Bioeng.* 35, 279 (1990).

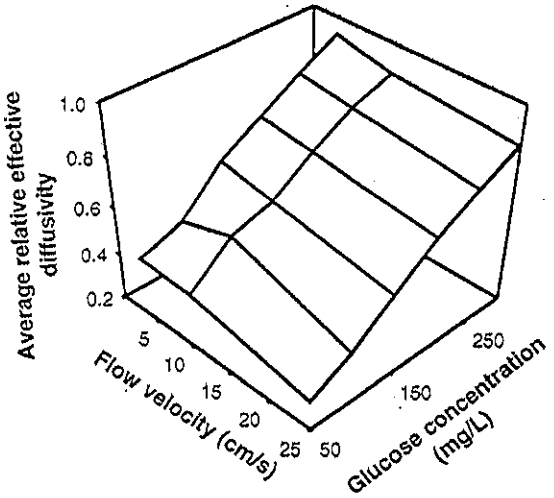

FIG. 10. The effects of growth conditions (bulk glucose concentration and average flow velocity) on the average relative effective diffusivity in biofilms. [Reproduced from H. Beyenal and Z. Lewandowski, *Wat. Res.* **34**, 528 (2000).]

Here D_a is average relative effective diffusivity of ferricyanide in the electrolyte or average relative effective diffusivity of growth limiting substrate in the medium, and X_f is average biofilm density (g/liter). This equation can be solved for the biofilm density as a function of the effective diffusivities measured in biofilm. Figure 11 shows that the average density of the biofilm near the bottom was on the order of 100 g/liter, which is consistent with observations reported by Zhang *et al.*[37] and Zhang and Bishop.[38]

Concluding Remarks

Limiting-current-type microelectrodes are remarkably versatile when applied to the measurement of mass transport rates in biofilms. Local mass transport coefficient, local effective diffusivity, and local flow velocity can all be measured. When the results of these measurements are superimposed on the results of nutrient uptake dynamics, the intricate interplay between mass transport dynamics and microbial activity in biofilms becomes visible, at least in simple experimental systems.

The most controversial part of the limiting current techniques, when applied to biological systems, is the choice of cathodic reactants. Ideally, such a reactant

[37] T. C. Zhang, Y. C. Fu, and P. L. Bishop, *Wat. Environ. Res.* **67**, 992 (1995).
[38] T. C. Zhang and P. L. Bishop, *Wat. Res.* **28**, 2279 (1994).

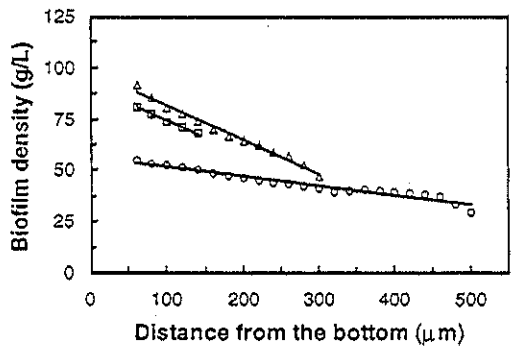

FIG. 11. Profiles of biofilm density in mixed population and pure culture *Pseudomonas aeruginosa* biofilms. ○, Mixed culture (v = 1.6 cm/s); △, mixed culture (v = 3.2 cm/s); □, *Pseudomonas aeruginosa* (v = 3.2 cm/s). [Reproduced from H. Beyenal, A. Tanyolaç, and Z. Lewandowski, *Wat. Sci. Tech.* **38**, 171 (1998).]

would not be toxic to the microorganisms, would not serve as a substrate in metabolic reactions, and would not react chemically with the biomass. At the same time it should exhibit acceptable electrochemical properties, reversible kinetics, and low overpotential on the selected electrode. It is difficult to find such a reagent! Potassium ferricyanide, the cathodic reactant that we use, is not an ideal reagent mainly because it reacts with the biomass. We bypass this problem by waiting long enough for the biomass to equilibrate with the ferricyanide, which essentially means until the reaction between the ferricyanide and biomass is completed. As a result, we need to assume that this reaction does not change the measured properties of the biofilms significantly.

Acknowledgments

The research was supported by the cooperative agreement EED-8907039 between the National Science Foundation and Montana State University.